PAPER Special Section on New Era of Satellite Communication/Broadcasting/Application Technologies

Maximum Positioning Error Estimation Method for Detecting User Positions with Unmanned Aerial Vehicle based on Doppler Shifts

Hiroyasu ISHIKAWA[†a)], ***Senior Member***, **Yuki HORIKAWA**[†], ***Nonmember***, ***and*** **Hideyuki SHINONAGA**[††], ***Fellow***

SUMMARY In the typical unmanned aircraft system (UAS), several unmanned aerial vehicles (UAVs) traveling at a velocity of 40–100 km/h and with altitudes of 150–1,000 m will be used to cover a wide service area. Therefore, Doppler shifts occur in the carrier frequencies of the transmitted and received signals due to changes in the line-of-sight velocity between the UAVs and the terrestrial terminal. By observing multiple Doppler shift values for different UAVs or observing a single UAV at different local times, it is possible to detect the user position on the ground. We conducted computer simulations for evaluating user position detection accuracy and Doppler shift distribution in several flight models. Further, a positioning accuracy index (PAI), which can be used as an index for position detection accuracy, was proposed as the absolute value of cosine of the inner product between two gradient vectors formed by Doppler shifts to evaluate the relationship between the location of UAVs and the position of the user. In this study, a maximum positioning error estimation method related to the PAI is proposed to approximate the position detection accuracy. Further, computer simulations assuming a single UAV flying on the curved routes such as sinusoidal routes with different cycles are conducted to clarify the effectiveness of the flight route in the aspects of positioning accuracy and latency by comparing with the conventional straight line fight model using the PAI and the proposed maximum positioning error estimation method.

key words: *unmanned aerial vehicle, Doppler shift, positioning accuracy index, maximum positioning error estimation method, curving flight model*

1. Introduction

In recent years, unmanned aircraft systems (UASs) have been studied and developed as the temporal communication systems for emergency and rescue services during disasters [1], [2]. In a typical UAS model, several UAVs, traveling at velocities of 40–100 km/h with altitudes in the range of 150–1,000 m with circular routes, are used to cover a wide service area and to provide continuous wireless communication services. Frequency bands of 2–5 GHz are used for the communication links and 5,030–5,091 MHz has been allocated for the transmission of UAV control signals, as per the WRC2012 standard [3]. In Japan, several frequency bands such as 2.4 GHz and 5.7 GHz are allocated to the unmanned mobile communications systems to provide high quality and long-distance image transmission services [4].

A UAV is composed of a transmitter and receiver to transfer the signals to/from terrestrial stations and terminals, and UAV's velocity is much higher than that of the user terminals. Therefore, a Doppler shift occurs in the carrier frequencies of the transmitted and received signals owing to the variations in the line-of-sight velocity between the UAV and the terrestrial terminals. By observing multiple Doppler shift values from different UAVs, it is possible to detect the position of the user that possesses a communication terminal for the UAS service [5]. This Doppler shift-based position-detection method is very simple and the user terminal would only be required to transmit a continuous wave (CW) at regular intervals.

For several years, the authors have been investigating methods for detecting the user position using multiple UAVs and have evaluated the positioning accuracy of the proposed position-detection method using up to three UAVs flying in circular, parallel, and figure-of-eight routes [6]–[8]. The simulation results and the Doppler frequency distributions confirmed that the positioning accuracy depends on the number and locations of the UAVs and other parameters, such as the flight route, the initial position, and the velocity of the UAVs. To express the influence of the constellation and the initial arrangement of the multiple UAVs on the position-detection accuracy, instead of the dilution-of-precision (DOP) method used for GPS [9], an absolute value of cosine of the inner product between two gradient vectors, in other words two tangent vectors, of the hyperboloid surface at an arbitrary point in the target area, named the positioning accuracy index (PAI), has been proposed [10], [11]. The PAI mitigates the computational complexity of the simulation in which the random location errors in UAVs are assumed [12]. By using the proposed PAI, computer simulations were conducted for two types of flying UAVs, namely, as a circularly orbiting model and a figure-eight route model to confirm the adequate fight model and the initial arrangement of two UAVs [8]. Although the PAI is very useful and accurate to investigate the relationship between the user position and the arrangement of UAVs, the index cannot provide the amount of the positioning error distance directly.

For focusing on the operation of the typical UAS [1], [2], the flight model of the UAV is assumed to be circularly orbits for providing continuous wireless communication services to the particular area on the ground. On the other hand, a single UAV should fly with a linearly route when the utilization purpose of the UAV is to search and rescue sufferers in the mountainous areas or disaster areas within a wide area in a short time. Therefore, it is needed to investigate the adequate flying models with linearly routes

Manuscript received October 1, 2019.
Manuscript revised February 10, 2020.
Manuscript publicized May 8, 2020.

[†]The authors are with Nihon University, Koriyama-shi, 963-8642 Japan.
[††]The author is with Toyo University, Kawagoe-shi, 350-8585 Japan.
a) E-mail: ishikawa.hiroyasu@nihon-u.ac.jp

DOI: 10.1587/transcom.2019CBP0007

and clarify the appropriate measurement interval of Doppler shift using the single UAV.

In this study, a maximum positioning error estimation method related to the PAI is newly presented to confirm the statistical and quantitative performance of the positioning error distance in the Doppler shift based position detection system using UAVs [13], [14]. Further, the computer simulations are conducted to clarify the relationship between a new flight route model for the purpose of lifesaving, in which a single UAV flying on the sinusoidal routes with different cycles comparing with a straight line route, and the user position detection accuracy is evaluated using the proposed maximum positioning error estimation method [15].

In Sect. 2, the concept model and the methodology for position detection based on observed Doppler shifts are briefly described. In Sect. 3, the definition of the positioning accuracy index is presented first, and then the methodology of the maximum positioning error estimation method is described in detail. In this section, the performance comparison of the maximum estimated positioning error and the simulation results are also presented to confirm the practicality of the proposed estimation method. In Sect. 4, the simulation models and simulation conditions are described. In Sect. 5, the cumulative distribution functions of the PAI and the maximum estimated positioning errors are derived by computer simulations. Based on the maximum estimated positioning errors, the preferable flight model and its related parameters are identified for the linearly flight route model with the single UAV. In Sect. 6, the results are summarized and directions for future studies are discussed.

2. Position Detection Based on Doppler Shifts

Figure 1 shows the configuration of the position-detection system with a single UAV by observing the Doppler shift at different local time $t = t_1$ and t_2. The UAV is assumed to fly at a constant velocity along with a curving flight route. The fixed user's positional vector $\boldsymbol{u}$ and the location vector of the UAV $\boldsymbol{U}(t_i)$ at the local time t_i $(i = 1, 2)$ are expressed as $\boldsymbol{u} = (x, y, z)$ and $\boldsymbol{U}(t_i) = (X(t_i), Y(t_i), Z(t_i))$, respectively, in three-dimensional XYZ orthogonal coordinates, in which the XY-plane is the ground and the Z coordinate represents the altitude. The velocity of the UAV is expressed as a vector, $\boldsymbol{V}(t_i) = \left(V_x(t_i), V_y(t_i), V_z(t_i)\right)$. The locations of the UAVs are monitored with high accuracy in real time by the terrestrial control station using the GPS receivers embedded in the UAVs. In the actual system, it is difficult to control the locations of the UAVs with high accuracy owing to the wind blowing and air currents. Furthermore, the transmission frequency of the transceivers embedded in the UAVs is assumed to be 5 GHz and the frequency offset caused by the oscillator with a stability of typically around 1 ppm in the user terminal is assumed to be pre-compensated precisely by using digital signal processing technologies such as the delay locked loop (DLL), the phase locked loop (PLL), and the combination of several types of frequency offset estimation and compensation methods [9]. Further, a constant frequency offset would be estimated by the least square algorithm [8] by assuming the frequency offset error included in the measured Doppler-shift as an unknown parameter which is the same as an unknown timing offset included in the measured TOA (Time of Arrival) in GPS caused by the clock error. However, the residual frequency errors remain in the measured Doppler-shift caused by the propagation channel and the instantaneous deviations caused by the receiver noise and so on. These measurement errors degrade the positioning accuracy of the proposed method depending on the environmental conditions and the receiver performance. In this paper, the influence of the above implementation issues to the position detection accuracy is treated as further research items so as to focus on the proposal of the maximum positioning error estimation method.

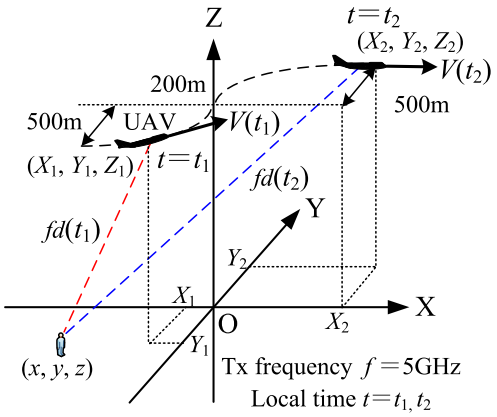

Fig. 1 Conceptual model for a position-detection system using a single UAV.

The proposed position detection procedure is as follows. First, the communication terminal held by the user sends a CW with a fixed frequency at the local time $t = t_1$ and t_2. As shown in Fig. 1, the UAV receives the CW and relays it to the terrestrial control station, where the Doppler shift frequency values of the signal is measured at each time. By these measurements, the control station estimates the user's position by applying the least-squares method to the Doppler shift frequency values, the location data of the UAV, and the velocity vectors of the UAV in the XYZ orthogonal coordinates.

The position-detection method is very simple and does not require synchronization between the user terminal and the UAV, which is mandatory for time-of-arrival (TOA)-based ranging systems such as GPS. The calculations involved in the position detection method are described as below.

First, the Doppler shift frequency value $fd(t_i)$ observed between the UAV and the user at local time t_i $(i = 1, 2)$ in the XYZ orthogonal coordinates is expressed as follows [8]:

$$\begin{aligned} fd(t_i) &= -\left(\boldsymbol{V}(t_i) \cdot \tilde{\boldsymbol{u}}(t_i)\right)/\lambda \\ &= -\frac{V_x(t_i)(X(t_i)-x)+V_y(t_i)(Y(t_i)-y)+V_z(t_i)(Z(t_i)-z)}{\lambda\sqrt{(X(t_i)-x)^2+(Y(t_i)-y)^2+(Z(t_i)-z)^2}}. \end{aligned} \tag{1}$$

where λ is the wavelength of the CW and $\tilde{\boldsymbol{u}}(t_i)$ is the Eigen vector, $(\boldsymbol{U}(t_i) - \boldsymbol{u}) / |\boldsymbol{U}(t_i) - \boldsymbol{u}|$, from the user position to the UAV at the local time t_i.

Here, the partially differentiate of the Eq. (1) with respect to x, y, z are shown as follows:

$$\frac{\partial fd(t_i)}{\partial x} = -\frac{-V_x(t_i)\, r(t_i) + (X_i(t) - x)\, s(t_i) / r(t_i)}{\lambda \{r(t_i)\}^2}. \quad (2)$$

$$\frac{\partial fd(t_i)}{\partial y} = -\frac{-V_y(t_i)\, r(t_i) + (Y_i(t) - y)\, s(t_i) / r(t_i)}{\lambda \{r(t_i)\}^2}. \quad (3)$$

, and

$$\frac{\partial fd(t_i)}{\partial z} = -\frac{-V_z(t_i)\, r(t_i) + (Z_i(t) - z)\, s(t_i) / r(t_i)}{\lambda \{r(t_i)\}^2}. \quad (4)$$

where $s(t_i)$ and $r(t_i)$ are given by the following equations, respectively.

$$s(t_i) = V_x(t_i)(X(t_i) - x) + V_y(t_i)(Y(t_i) - y) + V_z(t_i)(z(t_i) - z).$$

$$r(t_i) = \sqrt{(X(t_i) - x)^2 + (Y(t_i) - y)^2 + (Z(t_i) - z)^2}.$$

The Eqs. (2), (3) and (4) are to be used for deriving the gradient vector at local time t_i $(i = 1, 2)$, discussed in the next section.

Figure 2 illustrates the relationship between the Doppler shift distributions and the UAV location when the UAV is located at the center of the evaluation area with a velocity of 100 km/h in the positive direction of the X-axis and at an altitude of 200 m. Under these conditions, the maximum Doppler shift is nearly 463 Hz with the carrier frequency of 5 GHz. As shown in Fig. 2, the user locations at any positions would be on the hyperbolic lines those are determined based on the measured Doppler shifts. Therefore, the user location can be estimated as the intersection of multiple hyperbolic lines corresponding to the measured Doppler shifts between the user and the single UAV at different local time.

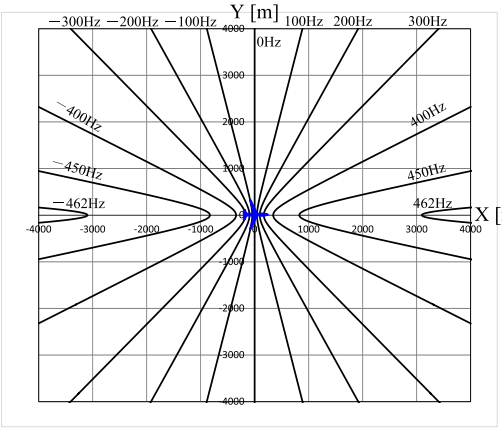

Fig. 2 Relationship between Doppler shift distributions and the UAV location.

3. Methodologies of Positioning Accuracy Index (PAI) and Positioning Error Estimations Related to PAI

3.1 Positioning Accuracy Index (PAI) Based on the Gradient Vectors Determined from the Doppler Shifts

Based on the results of the computer simulations in the previous works [6]–[8], it was confirmed that the positioning accuracy depends on the flight route, measurement time interval $\Delta t = t_1 - t_2$, and velocity of the UAV, and the relationship between the user position and the UAV location at each measurement time. To identify the best parameters, the PAI is applied to quantify the influence of the above conditions on the position detection accuracy, which calculated as the absolute value of cosine of the inner product between the two gradient vectors on the hyperboloid surface, each of which is formed based on a measured Doppler shift, at an arbitrary point (x, y, z) in the target evaluation area [9], [10]. Here, the gradient vector at local time t_i $(i = 1, 2)$ is expressed by the following:

$$\nabla fd(t_i) = \frac{\partial fd(t_i)}{\partial x}\boldsymbol{i} + \frac{\partial fd(t_i)}{\partial y}\boldsymbol{j} + \frac{\partial fd(t_i)}{\partial z}\boldsymbol{k}. \quad (5)$$

in which $\boldsymbol{i}$, $\boldsymbol{j}$ and $\boldsymbol{k}$ are the orthogonal unit vectors in the XYZ orthogonal coordinates.

Next, the absolute value of cosine of the inner product between two gradient vectors formed by Doppler shifts for the UAV at local time $t = t_1$ and t_2 at (x, y, z) is defined as follows:

$$|\cos\varphi_{12}| = \frac{|\nabla fd(t_1) \cdot \nabla fd(t_2)|}{|\nabla fd(t_1)|\,|\nabla fd(t_2)|} \quad (6)$$

where φ_{12} indicates the angle between the two gradient vectors. When the value of $|\cos\varphi_{12}|$ is close to 1 $(\varphi_{12} = 0, \pi)$, the two hyperbolic lines on the ground should be parallel at the user's position, as shown in Fig. 3(a).

Conversely, the two hyperbolic lines should be orthogonal when the value of $|\cos\varphi_{12}|$ is close to 0 $(\varphi_{12} = \pi/2)$ as shown in Fig. 3(b). In other words, the value of $\cos\varphi_{ij}$ represents the correlation between $\nabla fd(t_1)$ and $\nabla fd(t_2)$. Thus, it would be difficult to find the intersection between two hyperbolic lines when the absolute value $|\cos\varphi_{12}|$ is

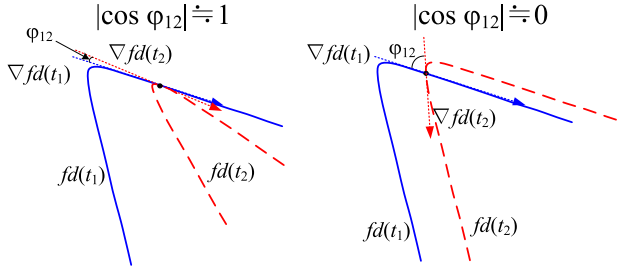

(a) low accuracy case (b) high accuracy case

Fig. 3 Relationship between the PAI and two hyperbolic lines based on the Doppler shifts.

close to 1, resulting in a large positioning error if the observed Doppler shifts include measurement errors. When the value of $|\cos\varphi_{12}|$ is close to 0, it would be easy to identify an intersection between the two hyperbolic lines even if the observed Doppler shifts include measurement errors. Ultimately, the Eq. (6) can be used to calculate the PAI to identify the best initial constellation and flight routes for the UAV to maximize the positioning accuracy in the target area. Furthermore, this index can be utilized to confirm the degree of reliability of the estimated user position derived by multiple Doppler shifts so as to avoid large positioning errors, as in the case with DOP for GPSs [9].

3.2 Maximum and Minimum Positioning Error Estimation Method Related to PAI

Next, an estimation method of maximum and minimum positioning errors based on the PAI is explained. Figure 4 indicates the relationship between the maximum and minimum estimated positioning errors and an angle of φ_{12} formed by two gradient vectors $\nabla fd(t_1)$ and $\nabla fd(t_2)$ when a hypothetical location error of the UAV is assumed to be a constant value of d [m] in the front-back direction. In this situation, as shown in Fig. 4, the estimated user position would be located in the green diamond shape area. Therefore, the maximum and minimum positioning errors, e_{max} and e_{mini}, are estimated as the Eqs. (7) and (8), respectively.

$$e_{max} = \frac{2d\cos(|\varphi_{12}|/2)}{\sin|\varphi_{12}|}, \tag{7}$$

$$e_{mini} = \frac{2d\sin(|\varphi_{12}|/2)}{\sin|\varphi_{12}|} \tag{8}$$

Figure 5 shows the characteristics of the maximum and minimum estimated positioning errors associated with the PAI, $|\cos\varphi_{12}|$, when the hypothetical location error d equals to 1 m for normalization. From this figure, the maximum estimated positioning error e_{max} increases in accordance with the value of $|\cos\varphi_{12}|$, and that value dramatically increases when $|\cos\varphi_{12}| > 0.9$. While, the minimum estimation error e_{mini} decreases from $\sqrt{2}$ m to 1 m in accordance with the value of $|\cos\varphi_{12}|$. As the flight location error of the UAV would be random, the user position detection error must be distributed up to e_{max} multiplied by a practical value of d.

In order to confirm the applicability of the proposed maximum positioning error estimation method, computer simulations were conducted and compared to the calculated maximum estimated positioning error. Figure 6 shows the model for computer simulation in which two isolated UAVs, indicated as "UAV1" and "UAV2", are flying in a circular route, a typical flight model for the UAS, with identical velocities of 100 km/h, radiuses of 500 m and altitudes of 200 m. Here, the distance between the centers of the circular orbits of the UAV1 and the UAV2 is 2 km. In this model, the UAV1 is assumed to start on the X-axis and the UAV2 starts at the initial phase angle of $\Delta\theta = 0°$, 45°, 90°, 135°, and 180°, respectively. The local time of the simulation was selected as 0 s, 28 s, 57 s, and 85 s. These values are selected to

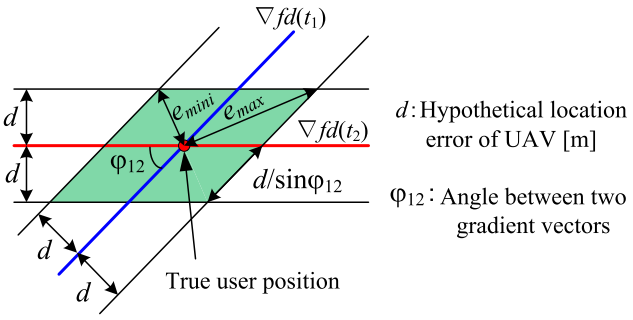

Fig. 4 Relationship between maximum and minimum estimated positioning errors and the angle φ_{12}.

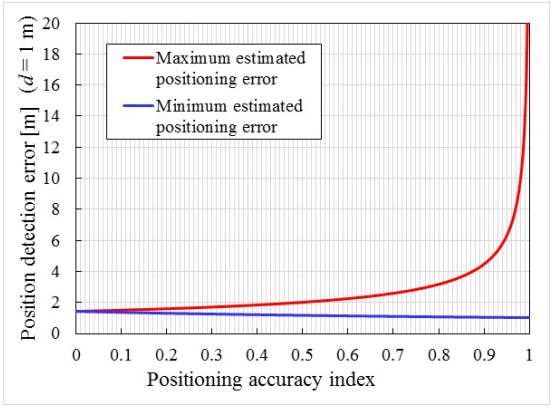

Fig. 5 Performance of the maximum and minimum estimated positioning errors associated with the PAI.

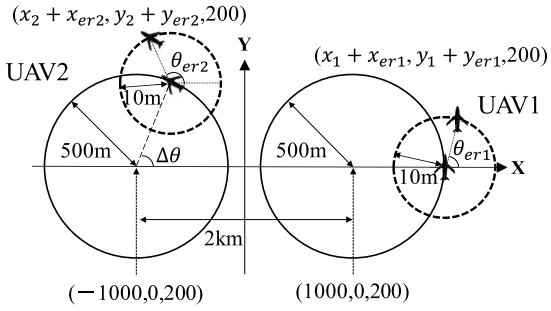

Fig. 6 Simulation model for evaluations of relationship between maximum positioning error and the PAI.

change the relationship between the locations of two UAVs and the velocity vectors of UAVs to be independent. Further, the location control error r_{er} of 10 m is artificially added in the flight position of the two UAVs on the XY plane independently by changing the plane angles θ_{er1} and θ_{er2} from 0° to 360° at intervals of 5°. Since the fundamental evaluation results were not affected, the control error on Z-axis was not considered in the simulation. Then, about 2,000 points evenly distributed in the range among $|\cos\varphi_{12}| = 0.0$ to 1.0 were selected in the area of 8 × 8 km on the XY-plane in the XYZ orthogonal coordinate system as an independent (x, y) coordination, where (x, y) is in the range between −4 km and +4 km on the X and Y axis, and computer

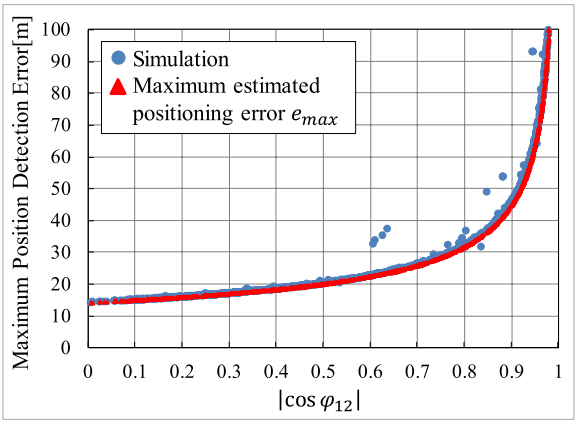

Fig. 7 Comparison of the maximum estimated positioning errors and simulation results associated with the PAI.

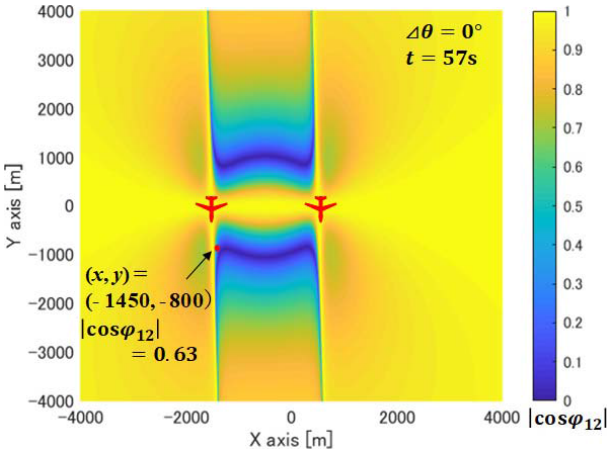

Fig. 8 Values of $|\cos\varphi_{12}|$ over the evaluation target area when $\Delta\theta = 0°$ and $t = 57$ s.

simulations based on the least square method [8] were conducted under the above conditions. In this case, a number of $(360°/5°)^2 = 72^2 = 5,184$ simulation results were produced at each (x, y) coordination and the maximum positioning error was selected and then plotted as a blue dot as shown in Fig. 7. In order to compare with the proposed maximum positioning error estimation method, the calculated results using the Eq. (7) are also plotted as a red regular triangle in Fig. 7. From this figure, it is confirmed that the simulation results and the calculated maximum estimated estimation error e_{max} shows a strong positive correlation and the cross-correlation value of them was approximately 0.947. Therefore, it can be concluded that the proposed maximum positioning error estimation method presents high accurate information of the positioning error without complex and time-consuming computer simulations.

Here, several simulation results exceed the theoretically estimated values because the user positions in the simulation were very close to the vertices of the hyperbolic lines that would be a borderline of two evaluation target areas where the position detection accuracy is very different [8]. Figure 8 shows an example of the error distribution in the position detection over the evaluation target area when $\Delta\theta = 0°$ and $t = 57$ s in Fig. 6. In this figure, the areas with high accuracy are indicated as blue and with low accuracy are as yellow corresponding to a value of the PAI. Further, it is confirmed that the large positioning errors occurred on the line that includes the directional vectors of the UAVs and on a straight line between the UAVs where the two hyperbolic lines are almost in parallel at the user position. In Fig. 8, a small red point near the border line is located at $(x, y) = (-1,450, -800)$ where the theoretical value of the PAI is 0.63 which is corresponding to the maximum estimated positioning error of about 23 m as shown in Fig. 7. However, the position detection error at this point in the computer simulation was about 38 m. This is because a 10 m of location control error of the UAV affects the simulation result of the least square method at such critical user points. Therefore, an incorrect convergence was occurred in the least square method depending on the location error of the UAV indicated in Fig. 8 near the borderlines of the positioning accuracy.

4. Simulation Model and Simulation Conditions

In the typical UAS [1], [2], the flight model of the UAV is assumed to be circularly orbits for providing continuous wireless communication services to the particular area on the ground. On the other hand, the UAV would fly with a linear route when the utilization purpose of the UAV is to search for and rescue sufferers in the mountainous areas or disaster areas within a wide area in a short time. Therefore, several types of the UAVs flying with linear routes are assumed in this study.

Figures 9(a), (b) and (c) show the three simulation models comprising a single UAV with velocity V of 100 km/h, i.e. $v = 27.78$ m/s, and an altitude of 200 m traveling in different patterns: a sinusoidal route with one cycle (**model A**), and a sinusoidal route with two cycles (**model B**) and a straight line route (**model C**), respectively. Here, the evaluation duration for the simulation is $T = 2\pi r/v$ where the distance $r = 500$ m. In this case, the UAV reaches at the distance of $R = 2,620.1$ m on the X-axis for model A and B, and 3,141.6 m for model C, respectively. The difference between models A and B is the changing rate of the velocity vectors of the UAVs and the changing cycles of the Doppler shifts. Thus, the location vector, $\boldsymbol{U}(t_i) = (X(t_i), Y(t_i), Z(t_i))$, for the models A and B can be expressed as shown in the Eqs. (9) and (10), respectively.

$$\begin{cases} X(t_i) = \int_{t_{A0}}^{t_{Ai}} v_{xA}(t)dt + X_{A0} \\ Y(t_i) = r\sin(\omega t_i) + Y_{A0} \\ Z(t_i) = Z_{A0} \end{cases} \tag{9}$$

$$\begin{cases} X(t_i) = \int_{t_{B0}}^{t_{Bi}} v_{xB}(t)dt + X_{B0} \\ Y(t_i) = r\sin(2\omega t_i) + Y_{B0} \\ Z(t_i) = Z_{B0} \end{cases} \tag{10}$$

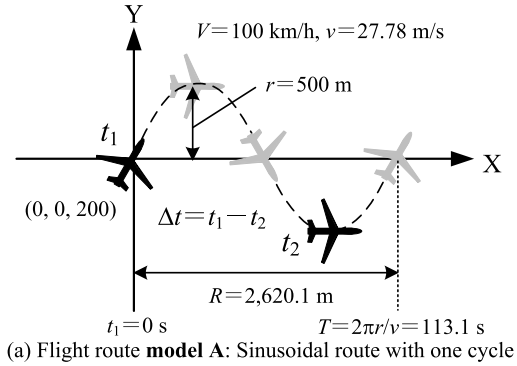

(a) Flight route **model A**: Sinusoidal route with one cycle

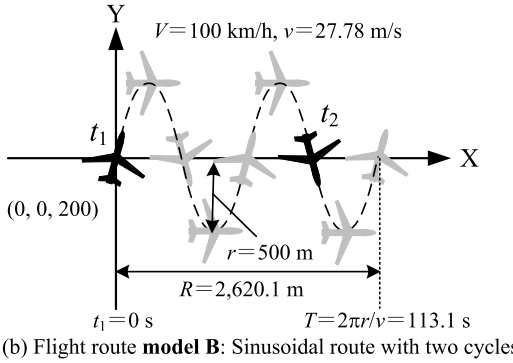

(b) Flight route **model B**: Sinusoidal route with two cycles

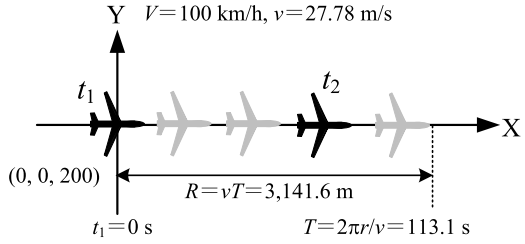

(c) Flight route **model C**: Straight line route

Fig. 9 Flight route models and related parameters for simulation evaluations.

Where, $v_{xA}(t) = v\cos\alpha$, $\alpha = \tan^{-1}(\cos\omega t)$, $v_{xB}(t) = v\cos\beta$, $\beta = \tan^{-1}(2\cos(2\omega t))$ and $\omega = v/r$. Here, the coordinates of (X_{A0}, Y_{A0}, Z_{A0}) and (X_{B0}, Y_{B0}, Z_{B0}) denote the start position of the UAV. In this study, the above parameters are set to be as $(X_{A0}, Y_{A0}, Z_{A0}) = (X_{B0}, Y_{B0}, Z_{B0}) = (0, 0, 0)$ and $t_{A0} = t_{B0} = 0$.

In the simulation, the area of 8×8 km on the XY-plane in the XYZ orthogonal coordinate system is assumed as "the evaluation target area" for the simulation. The four corners of the evaluation target area are $(-4,000\,\text{m}, -4,000\,\text{m})$, $(-4,000\,\text{m}, +4,000\,\text{m})$, $(+4,000\,\text{m}, -4,000\,\text{m})$, and $(+4,000\,\text{m}, +4,000\,\text{m})$. The distance between adjacent evaluation points is set to be 10 m such that there are $801 \times 801 = 641,601$ points for each simulation at the local time t.

5. Simulation Results

5.1 Relation Between the Position-Detection Error and the Positioning Accuracy Index

As reported in the previous works [6]–[8], the positioning accuracy changes with the flight route, the movement direction, the change rate of the velocity vector of UAVs, and the Doppler shift measurement interval Δt. Therefore, it is necessary to identify preferable parameters to make an effective and accurate position-detection system. In the simulation models A and B, the UAV moves sinusoidally in about 113.1 s and 56.5 s per a cycle, respectively. For the simulation model C, the same simulation duration of 113.1 s is set for comparison under the same simulation condition. In this case, the UAV reaches 3,141.6 meters away from the origin point toward the positive direction of X axis. To investigate the preferred flight route using a single UAV in the models A, B and C over time, the cumulative distribution function (CDF) of the PAI and the maximum estimated positioning error are calculated from all of the points in the target evaluation area at the time interval Δt of 7.1 s, equivalent to $\omega t = \pi/8$, to $\Delta t = 113.1$ s, equivalent to $\omega t = 2\pi$. In this case, the frequency for the CDF is 641,601 points as explained in Sect. 4.

Figures 10–12 show the CDF of the PAI, $|\cos\varphi_{12}|$, for flight route models A, B and C, respectively. In these figures, distributions of the PAI show the better performance when the CDF graph locates on the leftward side as explained in Sect. 3. From these figures, it can be confirmed that the CDF performance of the PAI improves in accordance with the increased Doppler shift measurement interval Δt since the distance between the location of the UAV at the local time $t = t_1$ and t_2 are getting longer. This feature was confirmed in the previous works also. In terms of the flight route models, some differences are observed when the measurement interval Δt are 7.1 s and 14.1 s. In these measurement intervals, the model B shows better performance compared to the models A and C, and the model C shows the worst performance. On the other hand, the model C shows the best performance when the measurement interval is more than 99.0 s.

5.2 Relation Between the Position-Detection Error and the Maximum Estimated Positioning Error

Next, Figs. 13–15 show the CDF of the maximum estimated positioning error e_{max} defined in the Sect. 3. From these figures, the same feature is confirmed, which observed for the PAI. Namely, the position detection accuracy is improved when the measurement interval is getting larger. In the case of the model B, there is a certain characteristic that the CDFs of $\Delta t = 14.1$ s, 21.2 s, and 28.2 s are nearly identical while in the models A and C are different. This feature would be caused that the model B is a flight route model with directions of the velocity vector changing rapidly. For the models A and B, the maximum estimated positioning errors between $\Delta t = 14.1$ s and 49.5 s show unstable performance compared to that of the model C and other measurement intervals because the flight direction of the UAV would exert influence on the position detection accuracy when the moved distance of the UAV's from the local time $t = t_1$ to t_2 is short.

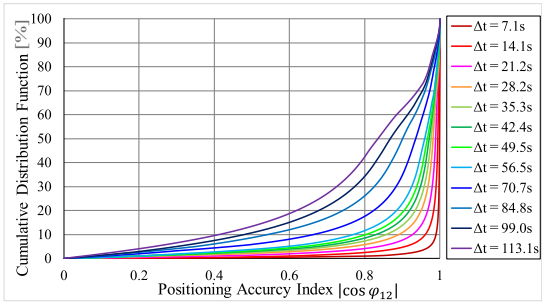

Fig. 10 CDF performance of the positioning accuracy index for **model A** with different measurement interval Δt.

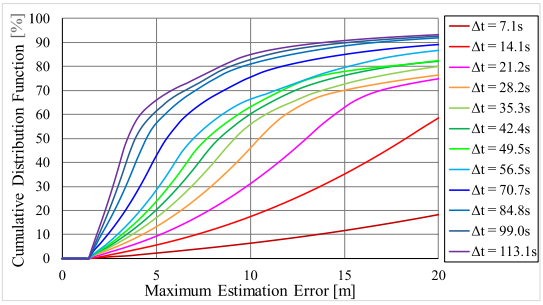

Fig. 13 CDF performance of the maximum estimated positioning error for **model A** with different measurement interval Δt.

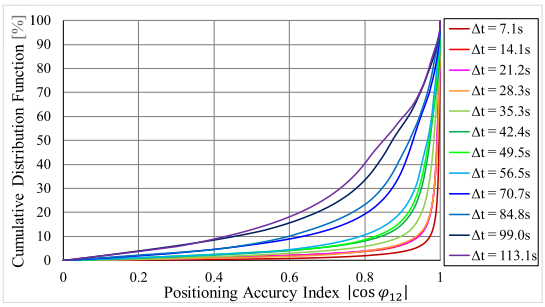

Fig. 11 CDF performance of the positioning accuracy index for **model B** with different measurement interval Δt.

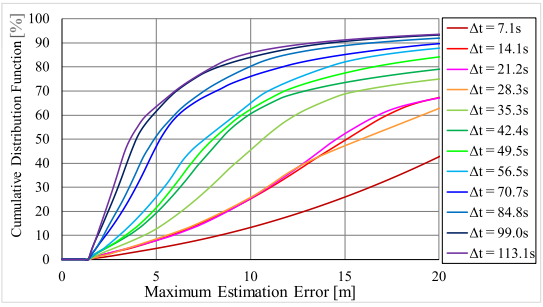

Fig. 14 CDF performance of the maximum estimated positioning error for **model B** with different measurement interval Δt.

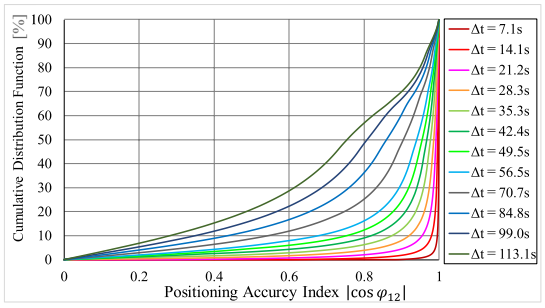

Fig. 12 CDF performance of the positioning accuracy index for **model C** with different measurement interval Δt.

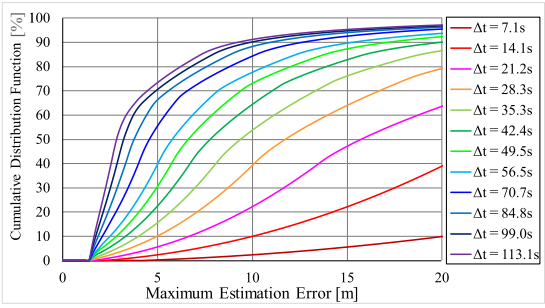

Fig. 15 CDF performance of the maximum estimated positioning error for **model C** with different measurement interval Δt.

To clarify the above features, the relationship between the maximum estimation error of the three flight route models and the Doppler shift measurement intervals Δt are indicated in Fig. 16 for the cases that the CDF of the three models are 50% and 90%. From this figure, it is confirmed that the model B shows the best position detection accuracy of less than 22 m compared to the models A and C, and the model C shows the worst performance when the measurement interval Δt is less than 14.1 s in the case of the CDF=50%. In order to confirm the above features, detailed performance evaluation was conducted in the range from Δt = 1 s to 12 s at intervals of 1 second and their results are shown in Fig. 17. From Fig. 17, it can be confirmed that the model B shows the best performance both for the CDF=50% and for the CDF=90%.

Conversely, as shown in Fig. 16, the model C shows the best performance especially for the CDF=90% when Δt is greater than approximately 20 s under the simulation conditions described in Sect. 4. This tendency is considered to come from that the distance from the initial to the ultimate positions of the UAV is longer than the other two models. Although the maximum estimation error for all the three models seems to be almost the same when the CDF=50% and Δt is getting longer, the model C shows the best performance also for the same reason.

For the models A and B, the maximum estimated positioning errors between Δt = 14.1 s and 49.5 s show unstable performance as mentioned before. Particularly, the model B shows a bad performance when Δt = 21.1 s in the case of CDF=90%. As discussed in Ref. [8], large positioning errors occurred in the areas which include the directional vectors of the UAVs and an extension of a straight line between the UAVs. In this particular case, the large positioning errors are resulted to spread over on the diagonal line in the eval-

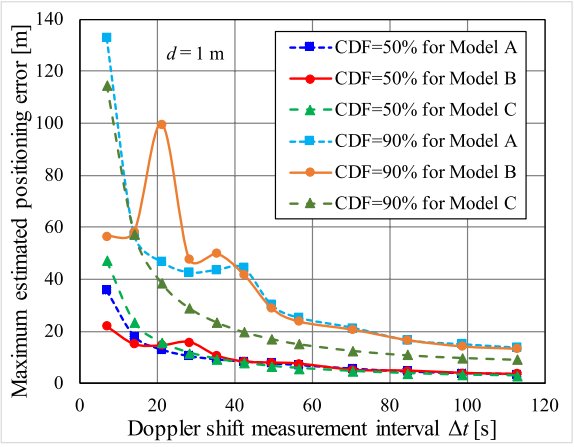

Fig. 16 Relationship between the maximum estimation error with CDF=50%&90% for the three models and the Doppler shift measurement interval Δt.

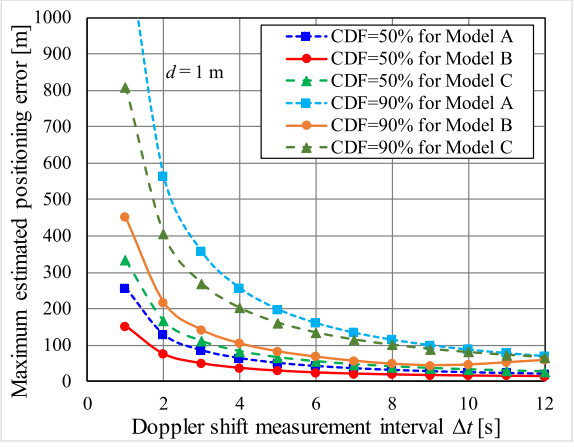

Fig. 17 Relationship between the maximum estimation error with CDF=50%&90% for the three models when the Doppler shift measurement interval Δt varies from 1 s to 12 s.

uation target area that comes from the relationship between the position and direction of the UAV at the local time $t = t_1$ and t_2. Therefore, the CDF performance was degraded as compared with the other Doppler shift measurement intervals.

From the above discussions, it can be concluded that the flight model B would be the appropriate for the position detection of the sufferers in a short time, and the model C would be the best flight model to achieve the higher positioning accuracy for the user position detection system using a single UAV.

6. Conclusion

In this study, the maximum positioning error estimation method related to the PAI was newly proposed to confirm the statistical and quantitative performance of the positioning error distance in the Doppler shifts based position detection system using UAVs. The performance comparison of the maximum estimated positioning error and the computer simulation results were also conducted. And it was confirmed that there is a strong positive correlation between them since the cross-correlation value showed approximately 0.947. Therefore, it can be concluded that the proposed maximum positioning error estimation method presents highly accurate information of the positioning error without complex and time-consuming computer simulations.

Further, the computer simulations were conducted to clarify the relationship between the new flight route model for the purpose of lifesaving, in which a single UAV flying on the sinusoidal routes with different cycles compared with a straight line route, and the user position detection accuracy was evaluated using the proposed maximum positioning error estimation method. From the simulation results, it was confirmed that the PAI and the maximum estimation error characteristics are depend both for the flight route models and the values of Doppler shift measurement interval. In particular, the CDF performances of the sinusoidal routes models show the better performance compared to that of the straight line flight model when the Doppler shift measurement interval is less than 20 s. Conversely, the straight line model shows the best positioning accuracy when the measurement interval is larger than 20 seconds. Therefore, it can be concluded that the curving flight model would be mainly appropriate for the urgent rescue of the sufferers, and the straight line route would be the best for achieving the higher positioning accuracy in the user position detection system using a single UAV.

In the future, further investigations will be conducted using the PAI and the maximum positioning accuracy estimation method with an aim of designing the best flight route not only for the single UAV system but also for the multiple UAVs system. Further, the environmental degrading conditions such as Doppler shift measurement errors caused by multipath signals, location control errors of the UAVs, frequency offsets produced in the oscillators and others are taken into account to clarify the practicality of the proposed position detection system using measured Doppler shift frequencies in the UAS.

Acknowledgments

This work was supported by JSPS KAKENHI, Grant Number 19K04380.

References

[1] R. Miura, K. Takizawa, M. Suzuki, H. Tsuji, M. Inoue, and Y. Owada, "Wireless relay using small unmanned aerial systems — For rapid recovery of network connection to isolated areas under large-scale disasters —," IEICE Technical Report, SAT2012-4, May 2012.
[2] K. Takizawa, H. Tsuji, M. Suzuki, and R. Miura, "Disaster-tolerant dependable wireless networks using unmanned aerial vehicles-on communications system design for UAV-to-UAV links," IEICE Technical Report, SANE2012-44, July 2012.
[3] N. Kadowaki, M. Toyoshima, A. Miura, S. Yamamoto, T. Takahashi,

N. Yoshimura, H. Tsuji, K. Takizawa, Y. Takayama, and Y. Munemasa, "Recent trends of satellite communication technologies applied to new frontiers," IEICE Trans. Commun. (Japanese Edition), vol.J97-B, no.11, pp.979–991, Nov. 2014.
[4] https://www.tele.soumu.go.jp/j/sys/others/drone/
[5] S. Kogure and H. Ishikawa, "Evaluation on user position detection method for unmanned aircraft system," IEICE Technical Report, WBS2014-18, July 2014.
[6] H. Ishikawa, "Study on user position detection method using one unmanned aerial vehicle," IEICE Technical Report, SAT2015-25, Aug. 2015.
[7] H. Ishikawa and H. Onuki, "Study on flight route of multiple unmanned aerial vehicles for user position detection method," IEICE Technical Report, SAT2016-65, Feb. 2017.
[8] H. Ishikawa, H. Onuki, and H. Shinonaga, "Method for detecting user positions with unmanned aerial vehicles based on doppler shifts," IEICE Trans. Fundamentals, vol.E102-A, no.1, pp.195–204, Jan. 2019.
[9] P. Misra and P. Enge, Global Positioning System: Signals, Measurements, and Performance, Ganga-Jamuna Press, Dec. 2010.
[10] H. Ishikawa, "Study on position accuracy index for user position detection method using unmanned aerial vehicles," IEICE Technical Report, SAT2017-3, May 2017.
[11] H. Ishikawa and H. Onuki, "Performance comparison of user position detection method using multiple unmanned aerial vehicles based on positioning accuracy index," IEICE Technical Report, WBS2018-3, March 2018.
[12] Y. Saito and H. Ishikawa, "Initial value selection algorithm for user position detection method based on sequential computation using unmanned aerial vehicles," IEICE Trans. Commun. (Japanese Edition), vol.J103-B, no.2, pp.119–129, Feb. 2020.
[13] H. Ishikawa, Y. Horikawa, and Y. Saito, "Positioning accuracy index for user position detection method using unmanned aerial vehicles," IEICE Communications Society Conference, BS-2-7, pp.S34–S35, Sept. 2018.
[14] Y. Horikawa and H. Ishikawa, "Performance evaluations of position detection method using unmanned aerial vehicles based on maximum positioning error estimation method," IEICE Technical Report, SAT2019-16, July 2019.
[15] H. Ishikawa, Y. Horikawa, and H. Shinonaga, "Performance evaluation of maximum estimation error of user position detection method using single unmanned aerial vehicle," IEICE Technical Report, SAT2019-64, Oct. 2019.

Hiroyasu Ishikawa received a B.E., M.E., and Ph.D. in Communication Engineering from Osaka University, Osaka, Japan in 1989, 1991, and 2001, respectively. He joined the Research and Development Laboratories of Kokusai Denshin Denwa Co., Ltd. (KDD) in 1991, where he has been engaged in the research of satellite navigation systems, mobile communication systems, and wireless LAN systems. He received the "Meritorious Award on Radio" from the Association of Radio Industries and Businesses in 2002 for the development of high-speed, long-distance wireless communications systems using the 2.4-GHz ISM band. Since April 2013, he has been a Professor at the College of Engineering, Nihon University, Fukushima, Japan.

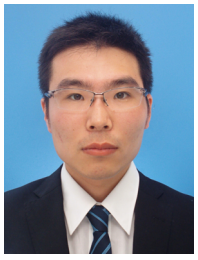

Yuki Horikawa received a B.E. in Electrical and Electronic Engineering from College of Engineering, Nihon University, Fukushima, Japan in 2018. He has been engaged in the research of user position detection system using UAVs. He is now a graduate student in Graduate Schools of Engineering, Nihon University.

Hideyuki Shinonaga received B.E., M.E., and D.E. degrees in Electrical Communications Engineering from Osaka University, Osaka, Japan, in 1979, 1981 and 1995, respectively. In 1981, he joined the Research and Development Laboratories of Kokusai Denshin Denwa (KDD, currently KDDI) Company, Tokyo, Japan, where he was been engaged in research on digital satellite communications, terrestrial radio systems, radio LAN's, ITS and digital cellular systems. He was an Executive Director of KDDI R&D Laboratories from 2002 to 2009. Since April 2009, he has been a Professor of Faculty of Science and Engineering, Toyo University, Saitama, Japan.